Further improvement in the variational many-body wave functions for light nuclei

Q. N. Usmani,* K. Anwar, and Nooraihan Abdullah
Institute of Engineering Mathematics, University Malaysia Perlis, Malaysia
(Received 21 June 2012; published 17 September 2012)

An improved variational ansatz is proposed and implemented for variational many-body wave functions for light nuclei with nucleons interacting through Argonne (AV_{18}) and Urbana IX (UIX) three-nucleon interactions. The new ansatz is based upon variationally distinguishing between the various components of the two-body Jastrow and operatorial correlations, which are operated upon by three-body and spin-orbit correlations. We obtain noticeable improvement in the quality of the wave function and lowering of the energies compared to earlier results. The new energies are $-8.38(1)$, $-28.07(1)$, and $-29.90(1)$ MeV for ^{3}H, ^{4}He, and ^{6}Li, respectively. Though, the present improved ansatz still fails to stabilize the ^{6}Li nucleus against a breakup into an α particle and a deuteron by 390 KeV; nonetheless, it is an improvement over previous studies.

DOI: 10.1103/PhysRevC.86.034323 PACS number(s): 21.60.Ka, 13.75.Cs, 21.10.Dr, 27.10.+h

I. INTRODUCTION

In an earlier publication, two of us (Q.N.U. and K.A.) proposed and implemented a simple method for improving the variational wave function of a many-body system [1]. In particular, we applied the method to lighter nuclei ^{3}H, ^{4}He, and ^{6}Li. The method was based upon improving the radial shape of the already-known correlations that were introduced over a number of years, relying primarily upon intuition and physical insight, and in part were guided by perturbation theory and various features of the shell model [2]. It was demonstrated that the relative error in the many-body wave function increases at least in proportion to the number of pairs of particles. Thus, as the number of particles in the system increases, the errors also grow. Our improvement of the wave function led to essentially exact solutions for nucleon interacting with central interactions [3,4] for ^{3}H, ^{4}He, ^{6}Li, and ^{6}He. But with nucleons interacting through realistic interactions, such as Argonne AV_{18} [5] two-body and Urbana UIX [6] three-body interactions, which have complicated operatorial dependence, the improved variational Monte Carlo (VMC) method gives only approximate solution [1]. Though, the improvement was significant, particularly for ^{6}Li [1], which was around 1.7 MeV (5.6%) lower compared to earlier VMC result [2], but it failed to provide a stable ^{6}Li against breakup into an α particle and a deuteron by 430 KeV. Improvements in ^{3}H and ^{4}He energies were 0.4% and 0.6%, respectively, though small but statistically significant. But the energies of ^{3}H, ^{4}He, and ^{6}Li were higher by 1.3%, 1.6%, and 4.7%, respectively, as compared to the effectively exact Green's Function Monte Carlo (GFMC) [2] calculations. In constructing the variational wave functions, we have used the known correlations and their structures as proposed and developed earlier by Pandharipande and collaborators [7–11], which we designate as PANDC correlations.

In the present work, we continue to use PANDC correlations but with a difference. We modify their structure somewhat. The state-of-the-art variational wave function for s- and p-shell nuclei consists of two parts: (a) a Jastrow part operated upon by a symmetrized sum of two-body operatorial correlations, and (b) this outcome is then operated by a sum of unity, operatorial three-body and spin-orbit two-body correlations. We now propose the ansatz that the outcome from (a) is variationally different for the three terms of (b); i.e., we have three variationally distinct Jastrow and the symmetrized sum of the two-body operatorial correlations each for unity, operatorial three-body and spin-orbit two-body correlations. This, in essence, is the main theme of this paper. This shall be elaborated in more details in the next section. Implementation of this ansatz then leads to a further lowering of energies of ^{3}H and ^{4}He by 0.4% and 0.6%, respectively. The improved energies for ^{3}H and ^{4}He become -8.38 and -28.07 MeV, respectively, which are significantly lower than the older VMC energies of -8.32 and -27.72 MeV [2]. But, the new, improved energies are still significantly higher compared to GFMC energies which are -8.46 and -28.34 MeV, respectively, for ^{3}H and ^{4}He. This clearly indicates that we are still missing some correlations in the present variational ansatz. With the new ansatz, however, lowering in the ^{6}Li energy is not much. It goes down from -29.69 [1] to -29.90 MeV, a relatively small decrease by 0.21 MeV. It still fails to stabilize ^{6}Li against a breakup into an α particle and a deuteron by 390 KeV. We do not resolve this problem here. We leave it for a future study.

In Sec. II, we briefly describe the Hamiltonian, i.e., Argonne AV_{18} and Urbana UIX interactions. In Sec. III, the wave function is described where we elaborate in details our present ansatz. In Sec. IV, we describe the results and discuss them. Section V is conclusions.

II. HAMILTONIAN

The Hamiltonian H consists of two- and three-nucleon potentials:

$$H = -\frac{\hbar^2}{2m}\sum_{i=1}^{A}\nabla_i^2 + \sum_{i<j}^{A} v_{ij} + \sum_{i<j<k}^{A} v_{ijk}. \qquad (2.1)$$

*Corresponding author: qamar@unimap.edu.com.my

For v_{ij}, we use the full Argonne AV_{18} [5] two-body potential, which is written as

$$v_{ij}(r) = \sum_{p=1}^{18} V_{ij}^{p}(r) O_{ij}^{p}. \tag{2.2}$$

The operators O_{ij}^{p} are given by

$$O_{ij}^{p=1-14} = [1, \vec{\sigma}_i \cdot \vec{\sigma}_j, S_{ij}, \vec{L} \cdot \vec{S}, L^2, L^2(\vec{\sigma}_i \cdot \vec{\sigma}_j), (\vec{L} \cdot \vec{S})^2] \otimes [1, \vec{\tau}_i \cdot \vec{\tau}_j], \tag{2.3}$$

$$O_{ij}^{p=15-18} = [1, \vec{\sigma}_i \cdot \vec{\sigma}_j, S_{ij}] \otimes T_{ij} \quad \text{and} \quad (\vec{\tau}_{zi} + \vec{\tau}_{zj}), \tag{2.4}$$

with $T_{ij} = 3\tau_{zi}\tau_{zj} - \vec{\tau}_i \cdot \vec{\tau}_j$ as the isotensor operator. All other symbols have their usual meanings. The first 14 operatorial components [Eq. (2.3) of Eq. (2.2)] are charge independent and are an updated version of Argonne AV_{14} potential [12]. The remaining four operators [Eq. (2.4)] consist of three charge-dependent and one charge-asymmetric operator. In addition, the potential consists of full electromagnetic interaction, containing the Coulomb, Darwin-Foldy, vacuum polarization, and magnetic moment terms with finite-size effects. The parameters of the potential have been obtained by fitting to the Nijmegen *pp* and *np* scattering data base [13,14], deuteron binding energy, and low-energy *nn* scattering parameters. For the three-nucleon potential, we use the Urbana IX model, which consists of two terms:

$$v_{ijk} = v_{ijk}^{FM} + v_{ijk}^{R}. \tag{2.5}$$

The Fujita and Miyazawa term [15] is given by

$$v_{ijk}^{FM} = \sum_{\text{cyc}} (A_{2\pi}\{\vec{\tau}_i \cdot \vec{\tau}_j, \vec{\tau}_i \cdot \vec{\tau}_k\}\{X_{ij}, X_{ik}\} + C_{2\pi}[\vec{\tau}_i \cdot \vec{\tau}_j, \vec{\tau}_i \cdot \vec{\tau}_k][X_{ij}, X_{ik}]), \tag{2.6}$$

where the symbols {} and [] stand for anticommutator and commutator terms and the operator X_{ij} stands for

$$X_{ij} = T_\pi(r_{ij}) S_{ij} + Y_\pi(r_{ij}) \vec{\sigma}_i \cdot \vec{\sigma}_j. \tag{2.7}$$

The v_{ijk}^{R} is a phenomenological spin-isospin-independent term:

$$v_{ijk}^{R} = U_0 \sum_{\text{cyc}} T_\pi^2(r_{ij}) T_\pi^2(r_{jk}). \tag{2.8}$$

For Urbana IX model, $A_{2\pi} = -0.02930$ MeV, $C_{2\pi} = A_{2\pi}/4$ MeV, and $U_0 = 0.0048$ MeV. The radial factors $T_\pi(r)$ and $Y_\pi(r)$, respectively, are associated with the tensor and Yukawa parts of the one-pion-exchange potential with a cut-off:

$$T_\pi(r) = \left(1 + \frac{3}{\mu r} + \frac{3}{(\mu r)^2}\right) \frac{\exp(-\mu r)}{\mu r} [1 - \exp(-cr^2)]^2, \tag{2.9}$$

$$Y_\pi(r) = \frac{\exp(-\mu r)}{\mu r} [1 - \exp(-cr^2)], \tag{2.10}$$

with $\mu = 0.7$ fm^{-1} and the cut-off parameter $c = 2.1$ fm^{-2}.

III. WAVE FUNCTION

The state-of-the-art variational wave function for light nuclei (*s*- and *p*-shell) are written in the form

$$|\Psi_V\rangle = \left[1 + \sum_{i<j<k} \left(U_{ijk} + U_{ijk}^{TNI}\right) + \sum_{i<j} U_{ij}^{LS}\right] \times \left[S \prod_{i<j} (1 + U_{ij})\right] |\Psi_J\rangle. \tag{3.1}$$

For details regarding the various symbols and components in the wave function Eq. (3.1), the reader is referred to Sec. III of Ref. [1]. As briefly explained in the introduction, we now write a more general ansatz:

$$|\Psi_V\rangle = \left[S \prod_{i<j} \left(1 + U_{ij}^{a}\right)\right] |\Psi_J^a\rangle + \sum_{i<j<k} \left(U_{ijk} + U_{ijk}^{TNI}\right) \times \left[S \prod_{l<m} \left(1 + U_{lm}^{b}\right)\right] |\Psi_J^b\rangle + \sum_{i<j} U_{ij}^{LS} \left[S \prod_{k<l} \left(1 + U_{kl}^{c}\right)\right] |\Psi_J^c\rangle, \tag{3.2}$$

where, the superscripts *a*, *b*, and *c* refer to variationally different sets of the operatorial product of the Jastrow and the symmetrized sum of products of the two-body operatorial correlations U_{ij}. The Jastrow wave function $|\Psi_J\rangle$ for *s*-shell nuclei has the form

$$|\Psi_J^z\rangle = \left[\prod_{i<j<k} f_{ijk}^{c}(\vec{r}_{ij}, \vec{r}_{jk}, \vec{r}_{ki}) \prod_{i<j} f_c^z(r_{ij})\right] |\Phi_A(JMTT_3)\rangle, \tag{3.3}$$

where z stands for *a*, *b*, or *c* of Eq. (3.2). The central correlations f_c^z and f_{ijk}^{c} are the central two- and three-body correlations with no spin or isospin dependence and Φ_A is an antisymmetrized spin-isospin state. For light *p*-shell nuclei, the structure of $|\Psi_J\rangle$ is much more complicated:

$$|\Psi_J^z\rangle = A\left\{\left(\prod_{i<j<k} f_{ijk}^{c} \prod_{i<j\leqslant k} f_{ss}^{z}(r_{ij}) \prod_{k\leqslant 4<l\leqslant A} f_{sp}(r_{kl})\right) \times \sum_{LS[n]} \left(\beta_{LS[n]} \prod_{4<l<m\leqslant A} f_{pp}^{LS[n]}(r_{lm}) \times |\Phi_A(LS[n]JMTT_3)_{1234:56\cdots A}\rangle\right)\right\}. \tag{3.4}$$

The operator A operates upon the total wave function to ensure antisymmetry. The two-body central correlation f_{sp} (between an *s*- and a *p*-shell nucleon) has the same behavior as f_{ss}^{a} (or f_c^a, between the two *s*-shell nucleons) at short distances but goes to unity at large distances to allow for cluster formation into an α and the rest of the nucleons. The variational parameters $\beta_{LS[n]}$ give weights to the various LS components of the single-particle wave functions. The central correlation $f_{pp}^{LS[n]}$ between the two *p*-shell nucleons and f_{sp}

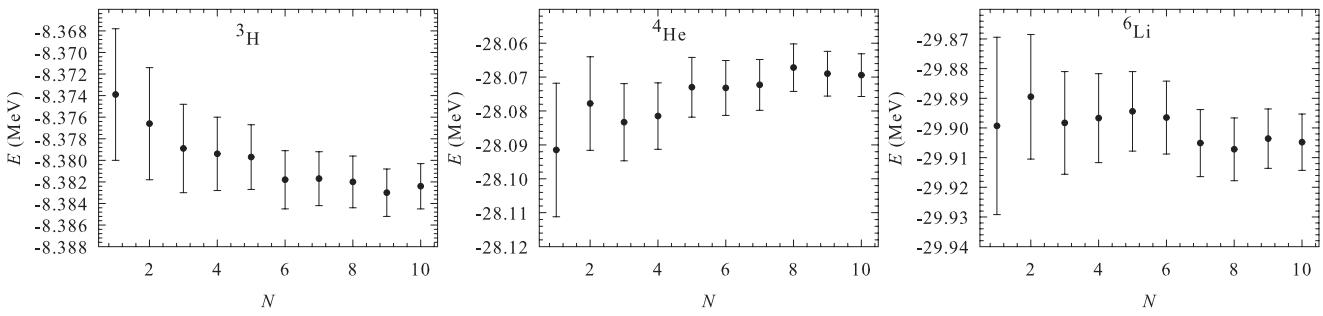

FIG. 1. Variational energies as a function of N, the number of configurations for the three nuclei. N has to be understood as $N \times 10^5$.

are assumed to have the forms

$$f_{pp}^{LS[n]} = f_c(r) + b_1^{LS[n]}\{1 - \exp[-(r/b_2^{LS[n]})^2]\}, \quad (3.5)$$

$$f_{sp}(r) = \frac{f_c(r)}{[1+\exp(r-s_1)]} + s_2\{1 - \exp[-(r/s_3)^2]\}, \quad (3.6)$$

where, $b_{1-2}^{LS[n]}$ and s_{1-3} are variational parameters. The single-particle wave function for the p-shell nucleons for different LS components is given by

$$|\Phi_A(LS[n]JMTT_3)_{1234:56\cdots A}\rangle = |\Phi_\alpha(0000)\rangle_{1234} \prod_{4<l\leqslant A} \phi_p^{LS[n]}(R_{\alpha l}) \times \left\{\left[\prod_{4<l\leqslant A} Y_{1m_l}(\Omega_{\alpha l})\right]_{LM_l[n]} \left[\prod_{4<l\leqslant A} \chi_l\left(\frac{1}{2}m_s\right)\right]_{SM_S}\right\}_{JM} \times \left[\prod_{4<l\leqslant A} \nu_l\left(\frac{1}{2}t_3\right)\right]_{TT_3}, \quad (3.7)$$

where $\Phi_\alpha(0000)$ stands for the antisymmetrized spin-isospin function of the α particle. The $\phi_p^{LS[n]}(R_{\alpha l})$ are the single-particle wave function of a p-shell nucleon, where $R_{\alpha l}$ is the relative distance of the nucleon from the center-of-mass of the α particle. χ and ν are the spin and isospin functions, respectively. The single-particle wave function $\phi_p^{LS[n]}(R_{\alpha l})$ are generated by assuming that the p-shell nucleon is moving in an effective Woods-Saxon potential, where the parameters of the potential have been treated as variational parameters [1,2].

The operators U_{ij}^z in Eq. (3.2) are sums of noncommuting spin, isospin, and tensor operators:

$$U_{ij}^z = \sum_{p=2,6}\left[\prod_{k\neq i,j} f_{ijk}^p(\vec{r}_{ij},\vec{r}_{jk},\vec{r}_{ki})\right] u_p^z(r_{ij}) O_{ij}^p. \quad (3.8)$$

The radial functions u_p^z are variationally different for z equal to a, b, or c. The operators O_{ij}^p are given by

$$O_{ij}^{p=2-6} = \vec{\tau}_i\cdot\vec{\tau}_j, \vec{\sigma}_i\cdot\vec{\sigma}_j, \quad (\vec{\sigma}_i\cdot\vec{\sigma}_j)(\vec{\tau}_i\cdot\vec{\tau}_j), \quad S_{ij} \quad \text{and} \quad S_{ij}(\vec{\tau}_i\cdot\vec{\tau}_j). \quad (3.9)$$

These are represented as τ, σ, $\sigma\tau$, t, and $t\tau$, and the corresponding u's are abbreviated as u_τ^z, u_σ^z, $u_{\sigma\tau}^z$,u_t^z, and $u_{t\tau}^z$, respectively. Together with f_c^z, they constitute a set of f_6^z correlations.

The three-body correlations U_{ijk} in Eq. (3.2) are induced by the two-nucleon interaction [11] and U_{ijk}^{TNI} are due to three-nucleon interaction. Variationally, these and the spin-orbit correlation U_{ij}^{LS} are treated here in exactly the same way as in Ref. [1]. The spin-orbit correlation consists of two terms:

$$U_{ij}^{LS} = \sum_{p=7,8}\left[\prod_{k\neq i,j} f_{ijk}^p(\vec{r}_{ij},\vec{r}_{jk},\vec{r}_{ki})\right] u_p(r_{ij}) O_{ij}^p,$$

$$O_{ij}^{p=7,8} = \vec{L}\cdot\vec{S}, \ \vec{L}\cdot\vec{S}(\vec{\tau}_i\cdot\vec{\tau}_j). \quad (3.10)$$

The u's, corresponding to $p = 7,8$, are denoted as u_b and $u_{b\tau}$, respectively. The f_c and seven u's (for $p = 2$–8) are obtained by minimizing the two-body cluster energy with a modified two-nucleon quenched potential [10]. Then f_c and five u's (for $p = 2$–6) provide the initial variational wave functions for Eqs. (3.2) to (3.4) for $z = a$, b, or c. These are variationally modified through the relations

$$f_c^z = f_c + \sum_{n=0}^{K} a_n^{c,z}\cos\left(n\pi r/r_d^{c,z}\right) \quad \text{for} \quad r \leqslant r_d^{c,z}, \quad (3.11a)$$

$$f_c^z = f_c \quad \text{for} \quad r \geqslant r_d^{c,z}, \quad (3.11b)$$

TABLE I. Variational energies and rms radii of various nuclei with AV_{18} + UIX potential. Results for ansatz Eq. (3.2) are for 1 million configurations.

Nucleus	Experiment		GFMC		VMC								
					Ansatz (3.1) Ref. [1]						Ansatz (3.2), Present		
	E(MeV)	$\langle r_p^2\rangle^{1/2}$	E(MeV)	$\langle r_p^2\rangle^{1/2}$	K	E(MeV)	$\langle r_p^2\rangle^{1/2}$	K	E(MeV)	$\langle r_p^2\rangle^{1/2}$	K	E(MeV)	$\langle r_p^2\rangle^{1/2}$
^{3}H	−8.482	1.60	−8.46(1)	1.59(0)	0	−8.32(1)	1.58(0)	7	−8.35(1)	1.58(0)	7	−8.38(0)	1.59(0)
^{4}He	−28.30	1.48(1)	−28.34(4)	1.45(1)	0	−27.72(4)	1.47(0)	7	−27.90(2)	1.44(0)	7	−28.07(1)	1.44(0)
^{6}Li	−31.99	2.43(4)	−31.15(11)	2.57(1)	0	−27.99(4)	2.48(0)	11	−29.69(3)	2.58(0)	11	−29.90(1)	2.52(0)

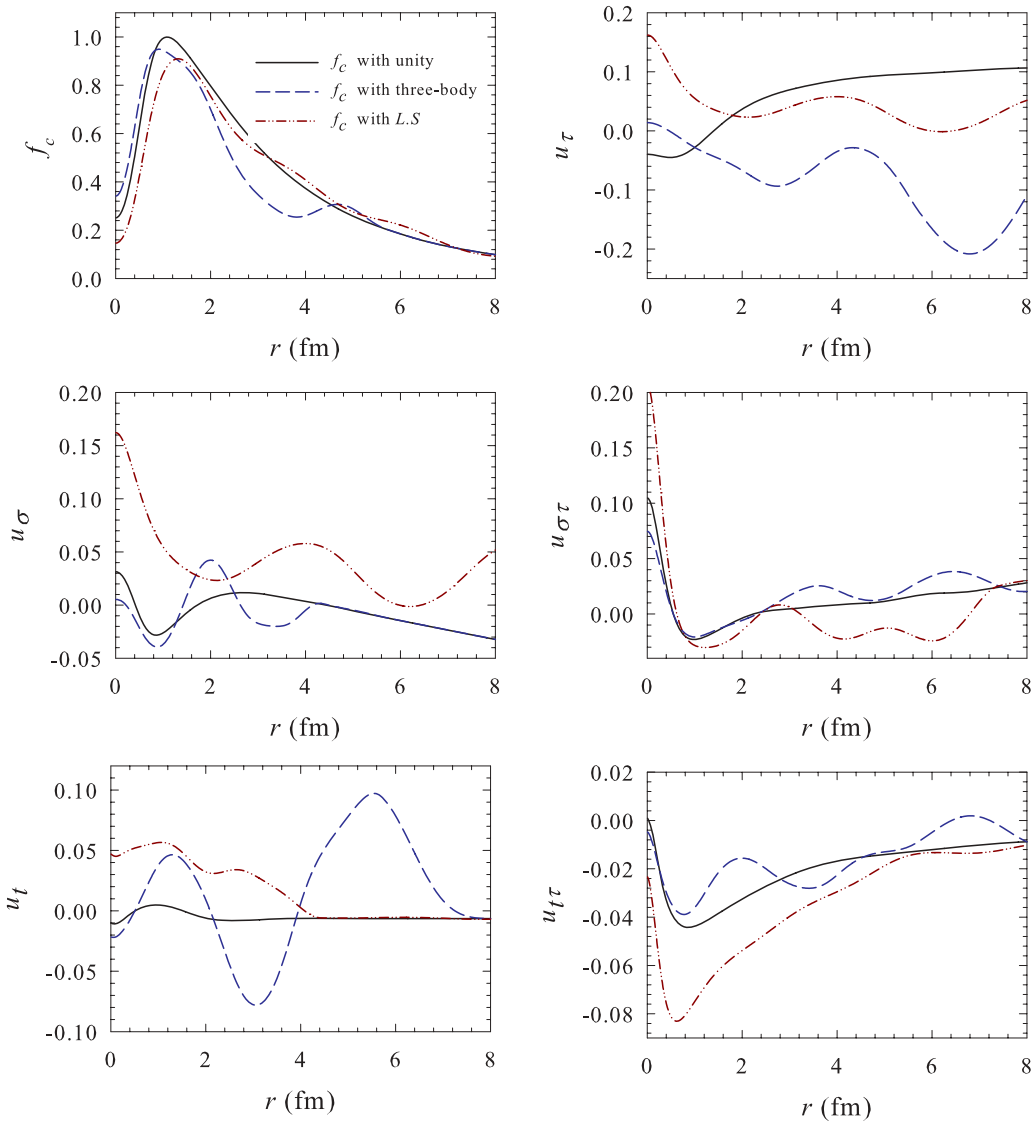

FIG. 2. (Color online) The f_6^a (black, solid line), f_6^b (blue, dashed line), and f_6^c (dark red, dash-dot-dot line) correlations for ^{3}H. For details see text.

$$u_p^z = u_p + \sum_{n=0}^{K} a_n^{p,z} \cos\left(n\pi r / r_d^{p,z}\right) \quad \text{for} \quad r \leqslant r_d^{p,z}, \tag{3.12a}$$

$$u_p^z = u_p \quad \text{for} \quad r \geqslant r_d^{p,z}, \tag{3.12b}$$

for $p = 2$–6. Here, $a_n^{c,z}$ and $a_n^{p,z}$ are variational parameters that are distinct for different z (a,b, or c). Similarly, the healing distances $r_d^{c,z}$ and $r_d^{p,z}$ are also variational parameters. At $r = r_d^{c(p),z}$, Eqs. (3.11) and (3.12) imply that

$$a_0^{c(p),z} = \sum_{n=1}^{K} (-1)^{n+1} a_n^{c(p),z}. \tag{3.13}$$

The cosine functions in Eqs. (3.11a) and (3.12a) also imply that the first derivatives of f_c^z and u_p^z at $r = r_d^{c(p),z}$ are zero. In all other correlations, modifications similar to Eqs. (3.11) or (3.12) have been employed without any z dependence [1].

IV. RESULTS AND DISCUSSION

The radial shape of the correlations Eqs. (3.11) and (3.12) are highly flexible in nature. With correlations of these type, a straightforward minimization of energy using a given but finite random set of Monte Carlo configurations invariably leads to very low values of the energy with large statistical errors. But with a new random walk with the optimized variational parameters the energy values become much higher. Thus, this procedure actually raises the true expectation value of the energy. We found it essential to minimize a suitable combination of energy and variance, σ, to find an upper bound on the energy. The variance is defined as

$$\sigma = \left[\frac{\langle H^2\rangle - \langle H\rangle^2}{N-1}\right]^{1/2}, \tag{4.1}$$

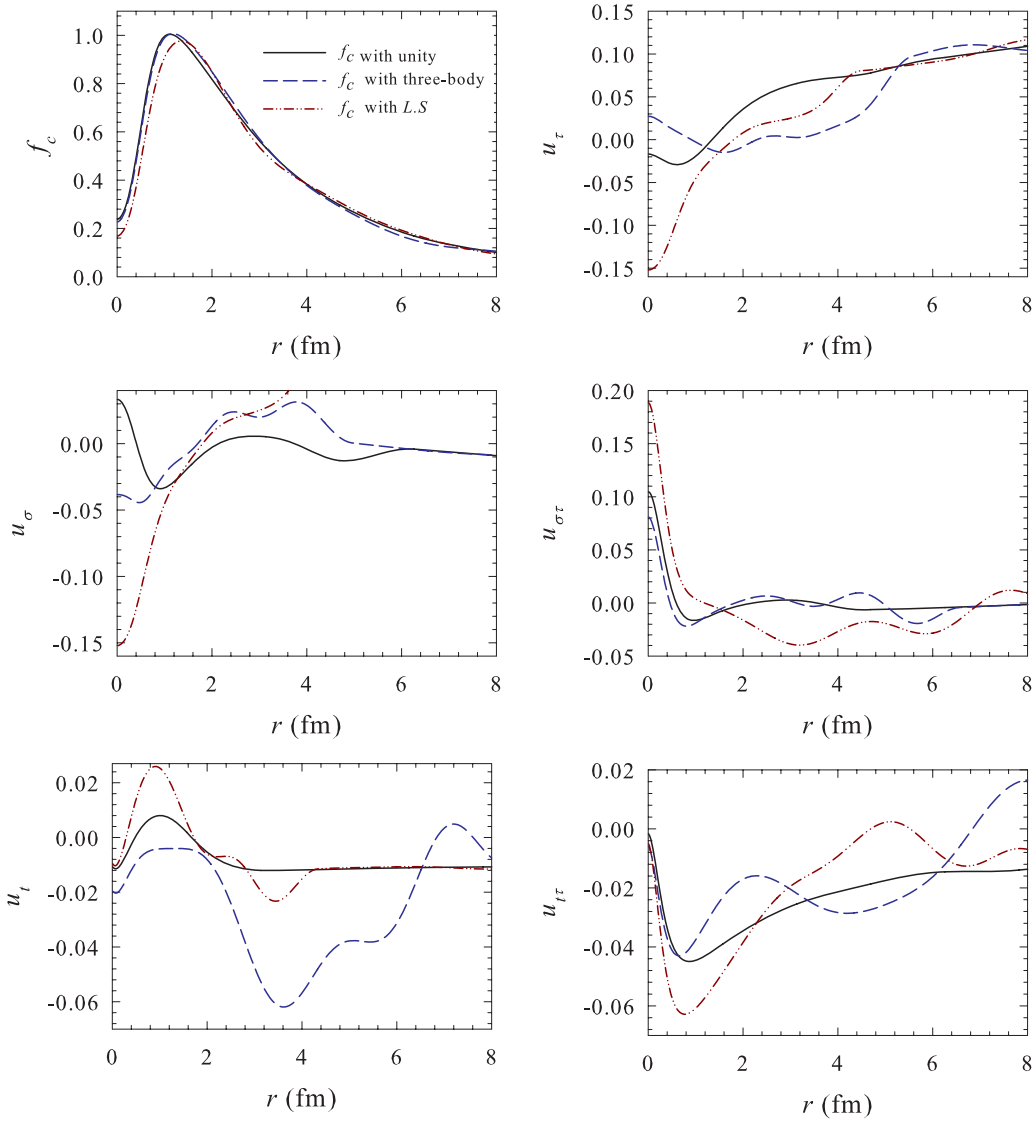

FIG. 3. (Color online) The f_6^a (black, solid line), f_6^b (blue, dashed line), and f_6^c (dark red, dash-dot-dot line) correlations for ^{4}He. For details see text.

where H is the Hamiltonian and N is the number of statistically independent samples. We, thus, minimize the function:

$$\chi = |E + C| + m_p(N-1)^{1/2}\sigma. \tag{4.2}$$

Here, E is the variational energy, obtained with the wave function described in Sec. III, and C is a positive constant much larger than $|E|$. The parameter m_p decides the relative importance of the energy and the variance in the minimization procedure. Its value is chosen through trial and is different for different systems. For ^{6}Li, because of the flexible nature of the correlations, the minimization of χ, [Eq. (4.2)], leads to very large values of the rms radius of this nucleus, which corresponds to its separation into an α and a deuteron cluster. To remedy this shortcoming we modify χ to

$$\chi(^6\text{Li}) = |E + C| + m_p(N-1)^{1/2}\sigma + n_p\left|\langle r^2\rangle_{\text{exp}}^{1/2} - \langle r^2\rangle_{\text{cal}}^{1/2}\right|, \tag{4.3}$$

where $\langle r^2\rangle_{\text{exp}}^{1/2}$ and $\langle r^2\rangle_{\text{cal}}^{1/2}$ are, respectively, the experimental and the calculated value of the rms radius of ^{6}Li, and, like m_p, the parameter n_p is a weight factor chosen by trial. Nonzero values of n_p are used at the initial stages of the minimization procedure. After a reasonable minimum is reached, we put $n_p = 0$ and search the variational parameters again. This procedure then gives a locally bound ^{6}Li nucleus without an α and a deuteron separable cluster.

In Table I, we present the results for ^{3}H, ^{4}He, and ^{6}Li. These were obtained with AV_{18} + UIX with full electromagnetic interaction. For comparison purposes results with earlier VMC [1] and GFMC [2] calculations are also given. The entries for $K = 0$ correspond to VMC calculations with PNADC correlations without any fine tuning, and for $K = 7$ for ^{3}H and ^{4}He, and $K = 11$ for ^{6}Li with fine-tuning using relations similar to Eqs. (3.11)–(3.13) as described in Ref. [1]. All these entries correspond to calculations with the ansatz Eq. (3.1). The last three columns give the results with the

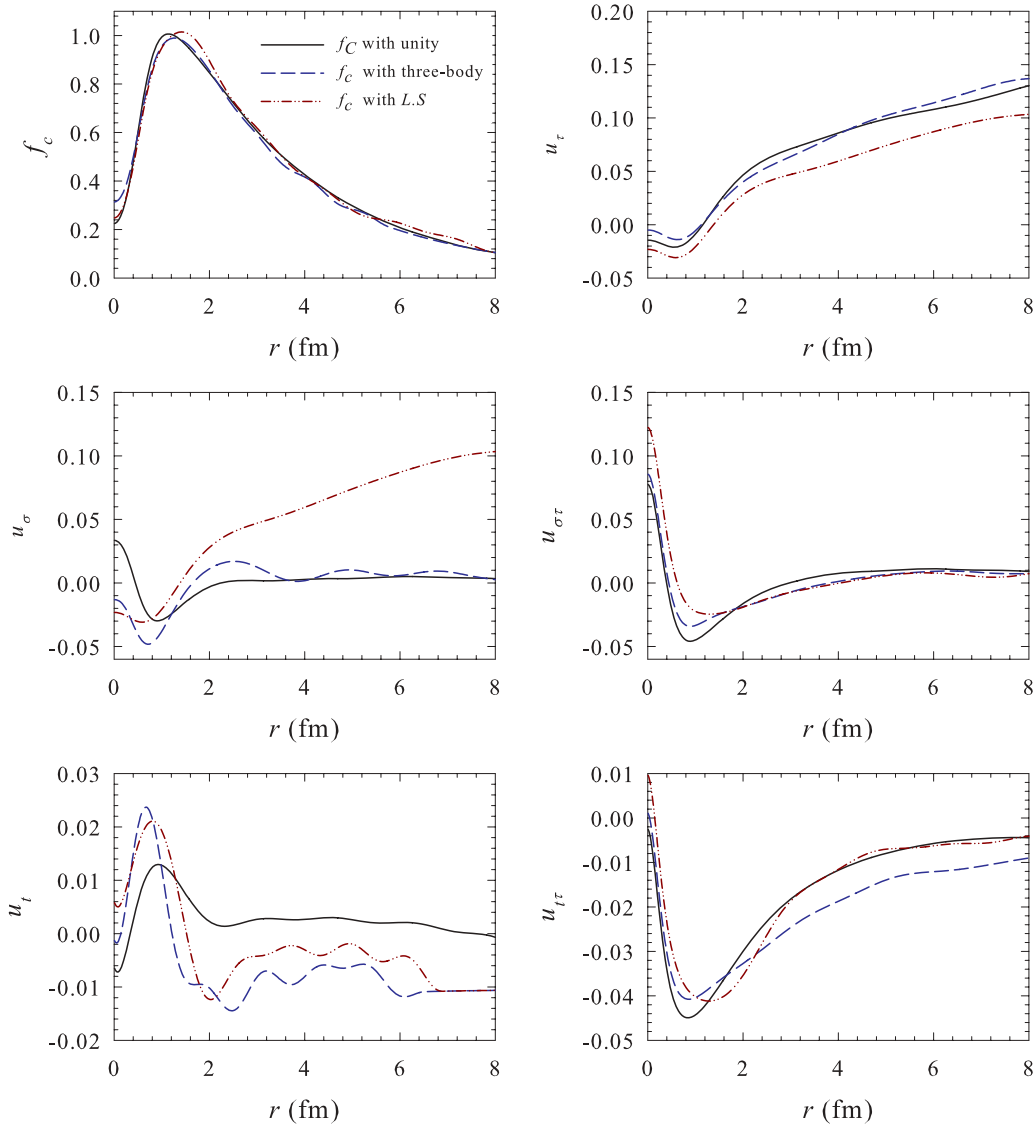

FIG. 4. (Color online) The f_6^a (black, solid line), f_6^b (blue, dashed line), and f_6^c (dark red, dash-dot-dot line) correlations for ^{6}Li. For details see text.

ansatz Eq. (3.2). The optimization of the energy was achieved by minimizing χ in the following manner. We begin with the wave function obtained with ansatz Eq. (3.1) and plug in this wave function into Eq. (3.2). We then vary the six correlations f_6^a using Eqs. (3.11)–(3.12) to minimize χ using Eq. (4.2) for ^{3}H and ^{4}He, and Eq. (4.3) for ^{6}Li. Next, f_6^b is

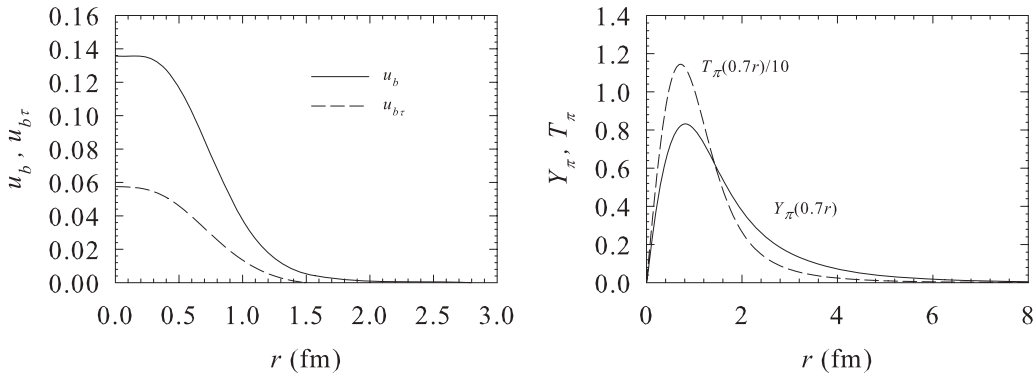

FIG. 5. (Left panel) The radial shapes of the spin-orbit correlations. (Right panel) The radial shapes of the functions appearing in the three body correlations.

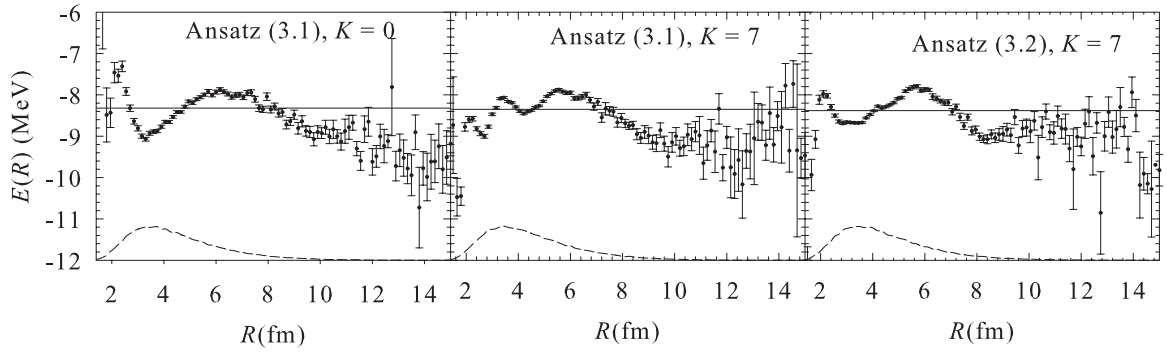

FIG. 6. Local energies for ^{3}H as a function of R. Left panel is with ansatz Eq. (3.1) without fine-tuning. Middle panel is with ansatz Eq. (3.1) with fine tuning. Right panel is with ansatz Eq. (3.2).

varied and then f_6^c. This process was iterated three times to achieve the final convergence through an automated procedure. The first iteration was carried out with 100 K predetermined random configurations with the best wave function at each stage of f_6^a,f_6^b, or f_6^c variations for ^{3}H and ^{4}He. For ^{6}Li, 10 K random configurations were used. In the next iteration, 200 K configurations for ^{3}H and ^{4}He were used; for ^{6}Li, 30 K configurations were employed. In the final iteration, 200 K configurations were increased to 300 K and 30 K to 50 K. For ^{6}Li, we performed one more iteration by putting $n_p = 0$ in Eq. (4.3) with the number of configurations 50 K. The results presented in Table I with the ansatz Eq. (3.2) are for 1 million configurations. In Fig. 1, we plot the variations in energy and variance for the three nuclei (left panel ^{3}H, middle panel ^{4}He, and right panel ^{6}Li) as a function of the number of configurations used starting from 100 K in steps of 100 K ending at 1 million configurations. This figure demonstrates that the variation of energy with respect to the number of configurations employed is small and is a good reflection on the quality of the wave function and the Monte Carlo evaluation. We shall elaborate on this more in the next paragraph.

Next, the question arises as to how do the f_6^z correlations differ from each other for $z = a$, b, or c, considering that this ansatz has lowered the energy for all three nuclei. In Figs. 2–4 we plot the $f_6^z(f_c^z, u_\tau^z, u_\sigma^z, u_{\sigma\tau}^z, u_t^z$, and $u_{t\tau}^z)$ correlations for $z = a$, b, and c for ^{3}H, ^{4}He, and ^{6}Li, respectively. Each figure pertains to one particular nucleus. The solid (black) line stands for f_6^a (with unity), the dashed (blue) line for f_6^b (with three-body), and the dash-dot-dot (dark red) line for f_6^c (with spin-orbit) correlations. We observe from the figures that all these correlations for $z = a$, b, and c are very different from each other. In addition, there are pronounced wiggles for $r \geqslant 2$ fm for $z = b$ (three-body, dashed curve) and c (spin-orbit, dash-dot-dot curve). For $z = a$ (unity, solid curve), all the correlations have more or less smooth behavior. In this case, both the short and the long range behavior of the correlations are important and contribute to energy. On the other hand, the three-body and spin-orbit correlations which operate upon f_6^b and f_6^c, respectively, are short-ranged. In the left panel of Fig. 5, we plot u_b and $u_{b\tau}$ as a function of r. It is seen that these correlations die out completely for $r < 2$ fm. In the right panel, we have plotted T_π $(0.7r)/10$ and Y_π $(0.7r)$ (the factor 0.7 being the variational scale factor), the radial shapes which appear in the three-body correlations [1]. They also become unimportant for $r \geqslant 3$ fm. Thus, to leading order of the cluster expansion of the wave function the wiggles in f_6^b and f_6^c shall be unimportant due to the short-ranged behavior of the three-body and spin-orbit correlations. Hence, these wiggles seem to have no physical origin or implications. They are probably a consequence of over-parameterization. In case, these unphysical wiggles were affecting the energy calculations, for example, through the higher-order components of the cluster expansion of the wave function, we would have probably felt their presence in the calculations through glitches appearing in the energy or the variance if the calculations were performed for a large number

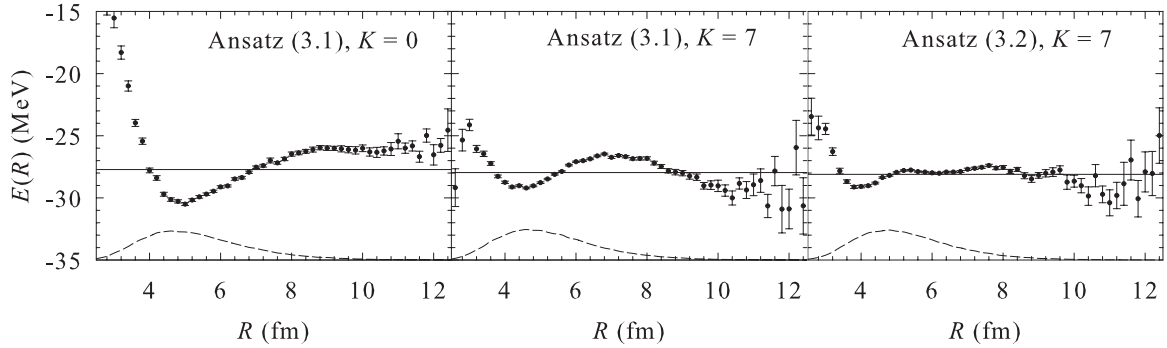

FIG. 7. Local energies for ^{4}He as a function of R. Left panel is with ansatz Eq. (3.1) without fine-tuning. Middle panel is with ansatz Eq. (3.1) with fine-tuning. Right panel is with ansatz Eq. (3.2).

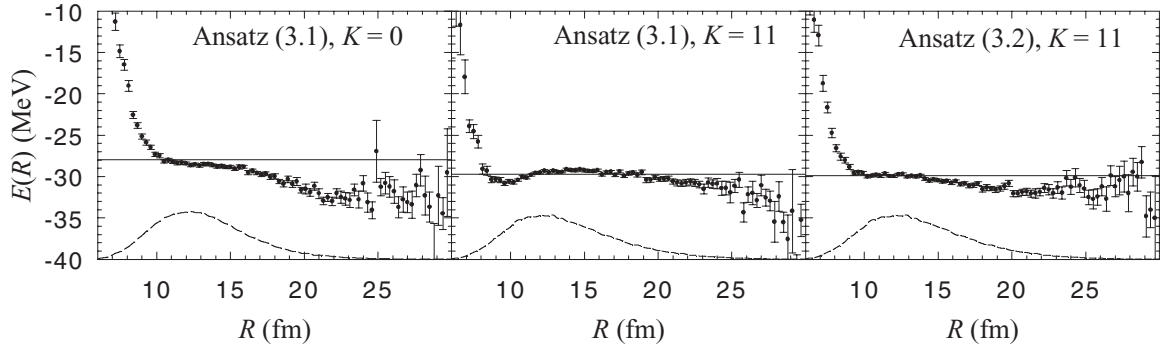

FIG. 8. Local energies for ^{6}Li as a function of R. Left panel is with ansatz Eq. (3.1) without fine-tuning. Middle panel is with ansatz Eq. (3.1) with tuning. Right panel is with ansatz Eq. (3.2).

of configurations. We see no such glitches in Fig. 1 for all the three nuclei. The energies are quite stable as a function of the number of configurations N and the variance is strictly proportional to $N^{-1/2}$ as a function of N. This is the reason that we carried out the calculations up to $N = 1$ million.

Another way of looking at the quality of the wave function is through the local energies $E(R)$ plotted as a function of R, where $R = \sum_i |r_i|$ with r_i being the distance of the ith nucleon from the center of mass. These energies and the corresponding variances are obtained by binning them around R with an interval of 0.1 fm. For an exact wave function Ψ, $E(R)$ will be independent of R. Thus, the variation of $E(R)$ as a function of R tells us about the quality of the wave function. In Figs. 6–8, we plot $E(R)$ as a function of R for ^{3}H, ^{4}He, and ^{6}Li, respectively. Left panels are the results of calculations with ansatz Eq. (3.1) without any fine-tuning of the wave function, middle panels are again with ansatz Eq. (3.1) but the wave functions are fine-tuned [1], and right panels are with ansatz Eq. (3.2). The lower dashed curves represent the relative probability of R occurrences in arbitrary units for 100,000 configurations. The solid straight lines represent the expectation values of the energies. We find that the variations of $E(R)$ from the solid line decreases steadily as we go from left to right panels. This decrease is particularly evident for ^{4}He (Fig. 7); for ^{3}H and ^{6}Li, the decrease is less pronounced (Figs. 6 and 8). It is fair to conclude that the ansatz Eq. (3.2) yields a better quality wave function. However, we are still above the GFMC values of energies by 0.08, 0.27, and 1.25 MeV for ^{3}H, ^{4}He, and ^{6}Li, respectively. In particular, we have not been able make ^{6}Li stable against a breakup into an α-particle and a deuteron, only a marginal improvement has been obtained with the ansatz Eq. (3.2) compared to the ansatz Eq. (3.1). We have to wait till new insight into the structure of the variational wave function is gained with complicated interactions such as AV_{18}.

V. CONCLUSIONS

In conclusion, we have made further progress with the variational wave functions of light nuclei. This became possible by considering different sets of variational f_6^z correlations when operated by three-body and spin-orbit correlations. Implementation of this additional flexibility in the wave function lead to a decrease in the energies of ^{3}H, ^{4}He, and ^{6}Li by 0.03, 0.17, and 0.21 MeV, respectively, as compared to the energies of Ref. [1]. Significant differences are found in the f_6^z correlations ($z = a$, b, or c) at short distances. It is argued that differences in the long-range behavior for $z = a, b$, or c are of no consequence because of the short-ranged nature of the three-body and spin-orbit correlations. We also demonstrated that the improved ansatz leads to an enhancement in the quality of the wave functions.

However, even with the improved ansatz, we do not find ^{6}Li stable against the decay into an α-particle and a deuteron. This stability is crucial, particularly if we want to extend the variational calculations for hypernuclei [16] in the p-shell region. We are continuing with our efforts in this direction.

ACKNOWLEDGMENTS

Q.N.U. is thankful to R. B. Wiringa and S. C. Pieper for helpful discussions. We gratefully acknowledge the Fundamental Research Grant Scheme (FRGS) No. 9003-00308, and the University Malaysia Perlis Grants No. 9014-00019 and No. 9001-00324.

[1] Q. N. Usmani, A. Singh, K. Anwar, and G. Rawitscher, Phys. Rev. C **80**, 034309 (2009).
[2] S. C. Pieper and R. B. Wiringa, Annu. Rev. Part. Sci. **51**, 53 (2001), and references therein.
[3] D. R. Thompson, M. LeMere, and Y. C. Tang, Nucl. Phys. A **286**, 53 (1977); I. Reichstein and Y. C. Tang, *ibid.* **158**, 529 (1970).
[4] R. A. Malfliet and J. A. Tjon, Nucl. Phys. A **127**, 161 (1969).
[5] R. B. Wiringa, V. G. J. Stoks, and R. Schiavilla, Phys. Rev. C **51**, 38 (1995).
[6] B. S. Pudliner, V. R. Pandharipande, J. Carlson, and R. B. Wiringa, Phys. Rev. Lett. **74**, 4396 (1995).
[7] V. R. Pandharipande, Nucl. Phys. A **174**, 641 (1971).

[8] J. Lomnitz Adler and V. R. Pandharipande, Nucl. Phys. A **342**, 404 (1980); J. Lomnitz Adler, V. R. Pandharipande, and R. A. Smith, *ibid*. **361**, 399 (1981).
[9] J. Carlson, V. R. Pandharipande, and R. B. Wiringa, Nucl. Phys. A **401**, 59 (1983).
[10] R. B. Wiringa, Phys. Rev. C **43**, 1585 (1991).
[11] A. Arriaga, V. R. Pandharipande, and R. B. Wiringa, Phys. Rev. C **52**, 2362 (1995).
[12] R. B. Wiringa, R. A. Smith, and T. L. Ainsworth, Phys. Rev. C **29**, 1207 (1984).
[13] J. R. Bergervoet, P. C. van Campen, R. A. M. Klomp, J. L. de Kok, T. A. Rijken, V. G. J. Stoks, and J. J. de Swart, Phys. Rev. C **41**, 1435 (1990).
[14] V. G. J. Stoks, R. A. M. Klomp, M. C. M. Rentmeester, and J. J. de Swart, Phys. Rev. C **48**, 792 (1993).
[15] J. Fujita and H. Miyazawa, Prog. Theor. Phys. **17**, 360 (1957).
[16] Q. N. Usmani, A. R. Bodmer, and Bhupali Sharma, Phys. Rev. C **70**, 061001(R) (2004); Rita Sinha, Q. N. Usmani, and B. M. Taib, *ibid*. **66**, 024006 (2002); Rita Sinha and Q. N. Usmani, Nucl. Phys. A **684**, 586c (2001); Q. N. Usmani and A. R. Bodmer, *ibid*. **639**, 147c (1998); Phys. Rev. C **60**, 055215 (1999).